AGU PUBLICATIONS

Geophysical Research Letters

RESEARCH LETTER
10.1002/2017GL075824

Key Points:
- We report the first statistical study on the duration of chorus elements
- The duration is longer at dayside and duskside than that at nightside and dawnside
- The duration is approximately inversely proportional to the frequency chirping rate

Correspondence to:
X. Tao,
xtao@ustc.edu.cn

Citation:
Teng, S., Tao, X., Xie, Y., Zonca, F., Chen, L., Fang, W. B., & Wang, S. (2017). Analysis of the duration of rising tone chorus elements. *Geophysical Research Letters*, *44*. https://doi.org/10.1002/2017GL075824

Received 25 SEP 2017
Accepted 30 NOV 2017
Accepted article online 4 DEC 2017

Analysis of the Duration of Rising Tone Chorus Elements

S. Teng[1,2], X. Tao[1,2], Y. Xie[1,2], F. Zonca[3,4], L. Chen[4,5], W. B. Fang[1,2], and S. Wang[1,2]

[1]CAS Key Laboratory of Geospace Environment, Department of Geophysics and Planetary Sciences, University of Science and Technology of China, Hefei, China, [2]Collaborative Innovation Center of Astronautical Science and Technology, China, [3]ENEA C. R. Frascati, Frascati, Italy, [4]Institute of Fusion Theory and Simulation and Department of Physics, Zhejiang University, Hangzhou, China, [5]Department of Physics and Astronomy, University of California, Irvine, CA, USA

Abstract The duration of chorus elements is an important parameter to understand chorus excitation and to quantify the effects of nonlinear wave-particle interactions on energetic electron dynamics. In this work, we analyze the duration of rising tone chorus elements statistically using Van Allen Probes data. We present the distribution of chorus element duration (τ) as a function of magnetic local time (MLT) and the geomagnetic activity level characterized by auroral electrojet (*AE*) index. We show that the typical value of τ for nightside and dawnside is about 0.12 s, smaller than that for dayside and duskside by about a factor of 2 to 4. Using a previously developed hybrid code, DAWN, we suggest that the background magnetic field inhomogeneity might be an important factor in controlling the chorus element duration. We also report that τ is larger during quiet times and shorter during moderate and active periods; this result is consistent with the MLT dependence of τ and the occurrence pattern of chorus waves at different levels of geomagnetic activity. We then investigate the correlation between τ and the frequency chirping rate (Γ). We show that, from observation, τ scales with Γ as $\tau \propto \Gamma^{-1.1}$, suggesting that statistically the frequency range of chorus elements ($\tau\Gamma$) should be roughly the same for different elements. These findings should be useful to the further development of a theoretical model of chorus excitation and to the quantification of nonlinear wave-particle interactions on energetic electron dynamics.

1. Introduction

Whistler mode chorus emissions are commonly observed electromagnetic plasma waves in the inner magnetosphere of Earth. Chorus consists of quasi-coherent discrete wave elements with frequency chirping (Burtis & Helliwell, 1975; Tsurutani & Smith, 1974). A power minimum around $0.5\Omega_{e0}$ is also frequently observed, forming lower and upper band chorus (Burtis & Helliwell, 1976; Tsurutani & Smith, 1974). Here Ω_{e0} is the electron cyclotron angular frequency at equator. These waves can effectively accelerate a few hundred keV electrons to MeV energies in the outer radiation belt (Horne et al., 2005; Reeves et al., 2013; Thorne et al., 2013) and cause precipitation of electrons from a few hundred eV to MeV energy range into the atmosphere, forming MeV electron microburst (Lorentzen et al., 2001; Kersten et al., 2011), diffuse aurora (Thorne et al., 2010), pulsating aurora (Nishimura et al., 2010), and pancake distributions (Meredith et al., 1999; Tao et al., 2011).

Previous research about chorus waves have mainly focused on two aspects. One is about the nature of wave-particle interactions between energetic electrons and chorus. Quasi-linear theory is typically used to model the global effects of these interactions. This approach, however, has been questioned because chorus elements are narrowband and quasi-coherent (Albert et al., 2012; Artemyev et al., 2012; Bell, 1984; Bortnik et al., 2008; Inan et al., 1978; Kellogg et al., 2010; Omura et al., 2007; Tao & Bortnik, 2010; Tao, Bortnik, Thorne, Albert, et al., 2012; Tao, Bortnik, et al., 2014), while in quasi-linear theory waves are assumed to be broadband so that particles move stochastically in phase space (Kennel & Engelmann, 1966). A coherent or quasi-coherent large-amplitude chorus element (Cattell et al., 2008; Wilson III et al., 2011) might lead to phase trapping or phase bunching of electrons, which cannot be described by quasi-linear theory. The other aspect of research about chorus focuses on its generation mechanism. Although it is widely accepted that this process is nonlinear (Helliwell, 1967; Nunn, 1971; Omura et al., 2008; Soto-Chavez et al., 2014; Tao et al., 2017a, 2017b; Trakhtengerts, 1995; Vomvoridis et al., 1982), more research is needed to develop a self-consistent theory about chorus excitation.

Relevant to both aspects of research are the detailed properties of chorus elements; for example, their amplitude, frequency chirping rate, the duration, and the period of repetition. These properties are needed in quantifying the nonlinear wave-particle interactions and in constraining theoretical chorus wave models. Some of these properties have been studied statistically using satellite data. Macúšová et al. (2010) and Tao, Bortnik, Thorne, Albert, and Angelopoulos (2012) used Cluster and Time History of Events and Macroscale Interactions during Substorms (THEMIS) observations, respectively, to test the relationship between chorus frequency chirping rate and several background plasma parameters. Shue et al. (2015) used THEMIS data to investigate the statistical distribution of the repetition period of rising tone chorus. Santolik, Nemec, et al. (2004) analyzed the subpacket period and its dependence on wave amplitude. Santolík et al. (2014) used Van Allen Probes data and studied fine structures of chorus elements including the subpackets and the instantaneous wave normal angle. In this work, we focus on the duration of chorus elements, which has never been studied before theoretically and observationally as far as we are aware of.

The remainder of the paper is organized as follows. We present our criteria of event selection, the method of data analysis and the distribution of our selected events in section 2. The dependence of duration on magnetic local time and the geomagnetic activity level, and the relation between duration and the frequency chirping rate are discussed in section 3. Our work is summarized in section 4.

2. Data Analysis

In this study, we use Van Allen Probes data from January 2014 to October 2015 during which the spacecraft complete one full precession (Kessel et al., 2013; Mauk et al., 2013) and therefore cover all magnetic local time (MLT). High time resolution measurements from burst mode of Electric and Magnetic Field Instrument Suite and Integrated Science (EMFISIS) (Kletzing et al., 2013) are used to investigate chorus element properties. These continuous waveform samples cover up to 6 s with a sampling rate of 35 kHz. We define each 6 s waveform data as a chorus event. Note that in our work, only Van Allen Probe A data are used.

To minimize the effects of wave propagation, we consider only events that are located within 3° in latitude, which is believed to be the boundary of the characteristic source region of chorus waves parallel to the magnetic field line (e.g., Santolik, Gurnett, et al., 2004). Then by visually inspecting the power spectrogram of each event, we select only events containing rising tone elements with clearly identifiable starting and ending frequencies. We limit our analysis to quasi-parallel propagating chorus waves to minimize the effect of wave normal angle. Only chorus elements with wave normal angle less than 40° are included. We further require that the starting frequency of the chorus element is smaller than $0.5f_{ce0}$, where $f_{ce0} \equiv \Omega_{e0}/2\pi$, but we do not limit the ending frequency to be less than $0.5f_{ce0}$. Therefore, a few selected events have chorus elements sweeping through $0.5f_{ce0}$.

Figure 1 (top) shows a typical chorus event used in this analysis. This event was observed by Van Allen Probe A from 19:15:02 to 19:15:08 UT on 30 April 2014. Color coded is the power spectral density (PSD) of the wave magnetic field. The observation was made at the magnetic latitude (MLAT) of −1.2°. The upper limit of y axis in Figure 1 is f_{ce0}. As can be seen, there are two bands in the event, but only the lower band is included in the analysis. An example of the visually determined starting and ending frequencies of a chorus element is shown. From the starting (t_1, f_1) and the ending points (t_2, f_2) of each element, the duration (τ) can be easily calculated as $\tau = t_2 - t_1$ and the frequency range $\Delta f = f_2 - f_1$ or $\Delta\omega = 2\pi\Delta f$. We also calculate the frequency chirping rate ($\Gamma \equiv \partial\omega/\partial t$) of each selected element to analyze the relation between τ and Γ. To calculate Γ, we search for the peak PSD along the line from the starting point to the ending point. A linear regression using the points of peak PSD gives the frequency chirping rate of the element. Note that, for a given event, not all elements are selected, because frequently, elements in the same event show similar properties such as the chirping rate. We typically choose 6–10 clear and distinguishable representative elements from each event.

Using the selection criteria above, we find in total 458 chorus events, from which we select 3,577 chorus elements. The distributions of all selected events in MLT, L shell and MLAT are shown in Figure 1 (bottom). Here the MLT, MLAT, and L shell parameters are calculated using the TS04 magnetic field model (Tsyganenko & Sitnov, 2005). Color coded is the average value of the element duration for each event. We use the average value of the duration here, because each event consists of several different elements and the location information (MLT, MLAT, and L) for all elements within a given event is the same. There are more nightside (MLT from 21 h to 0 h to 3 h) and dawnside (3 h $\leq$ MLT $<$ 9 h) events than dayside (9 h $\leq$ MLT $<$ 15 h) and duskside (15 h $\leq$ MLT $<$ 21 h) events. These features are related to the properties of chorus wave excitation

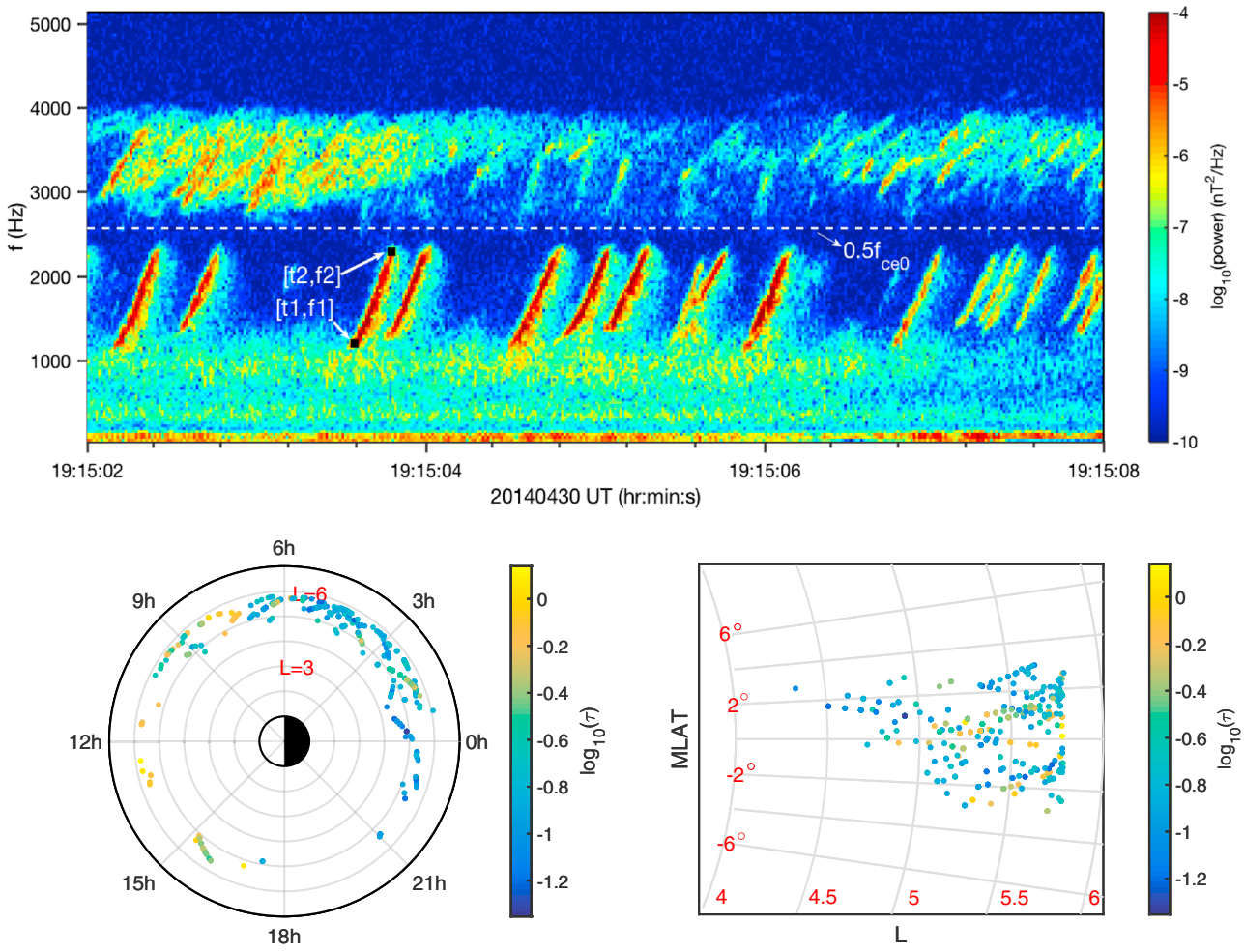

Figure 1. (top) An example frequency-time spectrogram of the power spectral density of magnetic field fluctuations observed on 30 April 2014 starting from 19:15:02 UT (L = 5.2, MLT = 8.9 h, MLAT = −1.2°). (bottom) The distribution of selected chorus events as a function of (left) MLT and L and (right) MLAT and L. Color coded is the logarithm of the average value of the duration of selected chorus elements within each event.

and the trajectory of Van Allen Probes. The distribution in the L-MLT domain, Figure 1 (bottom left), shows strong day-night asymmetry in the chorus element duration. Chorus elements from dayside and duskside typically last longer than those from nightside and dawnside. This feature will be analyzed in detail in the next section. Figure 1 (bottom right) shows the event distribution in L-MLAT domain. As mentioned in the criteria of event selection, all selected chorus events are located within $|\mathrm{MLAT}| \leq 3°$. The L shell range of the selected chorus elements is limited to $4 < L < 6$, and most elements are located between $L = 5$ and 6. Because of the narrow L shell coverage, the L shell dependence of τ is not clear from this data set. Therefore, in the following analysis, we will focus on the dependence of τ on MLT and the geomagnetic activity level characterized by the AE index.

3. Results

3.1. The Dependence of τ on MLT

In this section, we analyze the MLT dependence of the chorus element duration. We divide MLT into four sectors: nightside, dawnside, dayside, and duskside as described in the previous section. Figures 2a and 2b show the normalized histogram of τ for all four groups. There are in total 1,645 nightside elements, 1,436 dawnside elements, 163 dayside elements, and 333 duskside elements. The distributions of τ of nightside and dawnside chorus elements have a pronounced peak at about 0.12 s. On the other hand, the duration of dayside and duskside elements has a much wider distribution. The duration of most dayside elements is between 0.25 s and 0.8 s, while that of duskside elements is between 0.15 s and 0.55 s. The τ distribution

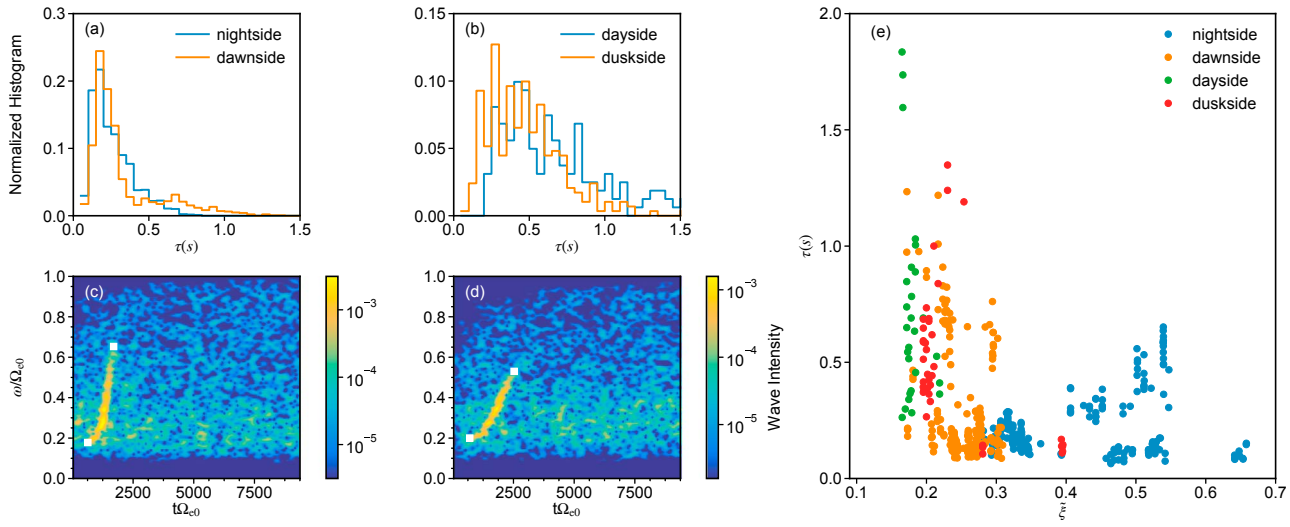

Figure 2. Normalized histogram of the duration of chorus elements from (a) nightside and dawnside, and (b) dayside and duskside. DAWN code simulation of chorus for (c) $\xi = \xi_N$ and (d) $\xi = \xi_D$. The white markers in Figures 2c and 2d indicate the starting and ending points of the elements. (e) The averaged τ for a given event as a function of the inhomogeneity factor calculated using the TS04 magnetic field model.

of dayside elements peaks at about 0.4 s, while that of duskside peaks at about 0.25 s. Therefore, in general, chorus elements from dayside and duskside last longer by about a factor of 2 to 4 than those from nightside and dawnside.

One possible reason for the day-night asymmetry in the τ distribution might be the asymmetry in the background magnetic field inhomogeneity (Tao, Lu, et al., 2014), which has been shown to play an important role in determining the frequency chirping rate of chorus elements (Helliwell, 1967; Tao et al., 2012) and the minimum threshold condition for chorus excitation (Keika et al., 2012; Tao, Lu, et al., 2014; Spasojevic & Inan, 2010). Because of the compression of the magnetosphere by solar wind, dayside magnetosphere has a smaller inhomogeneity factor near the equator than nightside for a given L. This results in a smaller frequency chirping rate and a lower threshold linear growth rate to excite chorus at dayside than at nightside. It is therefore possible that the day-night asymmetry in τ is also related to the asymmetry in the background magnetic field inhomogeneity.

To verify this conjecture, we first perform simulations of chorus using previously developed 1-D hybrid code DAWN (Tao, 2014). In this code, the background magnetic field is parabolic, $B = B_0(1 + \xi z^2)$, to approximate the magnetic field near its minimum (typically the magnetic equator), which is the source region of chorus. Here B is the magnetic field strength, $B_0 = B(z = 0)$, and z is the distance along a field line from the equator. The parameter ξ characterizes the inhomogeneity of the background magnetic field, and $\xi = 4.5/(LR_p)^2$ for a dipole field, where R_p is the planet radius. There are two components in the electron distribution: a cold component and a hot component with bi-Maxwellian distribution. The cold component is modeled using fluid equations, and the hot component is modeled using particle-in-cell techniques, following Katoh and Omura (2007). For other details of the DAWN code, we refer readers to Tao (2014).

We perform two simulations with $\xi_D = 2.16 \times 10^{-5} c^2 \Omega_{e0}^2$ and $\xi_N = 8.62 \times 10^{-5} c^2 \Omega_{e0}^2$. The subscript "D" ("N") means that the corresponding ξ is chosen to represent the dayside (nightside) magnetosphere. The simulation parameters are the same as those used by Tao, Lu, et al. (2014), who investigated the role of day-night asymmetry in determining the minimum linear drive to excite chorus. For simplicity, we only list the most relevant parameters here. The temperature anisotropy used in both simulations is $A \equiv T_\perp/T_\parallel - 1 = 2.06$. Here T denotes hot electron temperature, and subscripts "$\perp$" ("$\parallel$") the direction with respect to the background magnetic field. The ratio of the hot to cold electron number density for ξ_N is 1.53%, and that for ξ_D is 0.6%. To find the exact number of hot electron number density (n_h) for a given ξ, we fix A and perform a series of simulations, increasing n_h step by step until chorus elements are generated. Therefore, these chosen parameters (A and n_h) give the minimum linear growth rate to excite chorus waves for the two ξs. We use the same temperature anisotropy in the two simulations because observations (Li et al., 2010) show that temperature anisotropy at dayside might be comparable to that at nightside due to pitch angle scattering of electrons

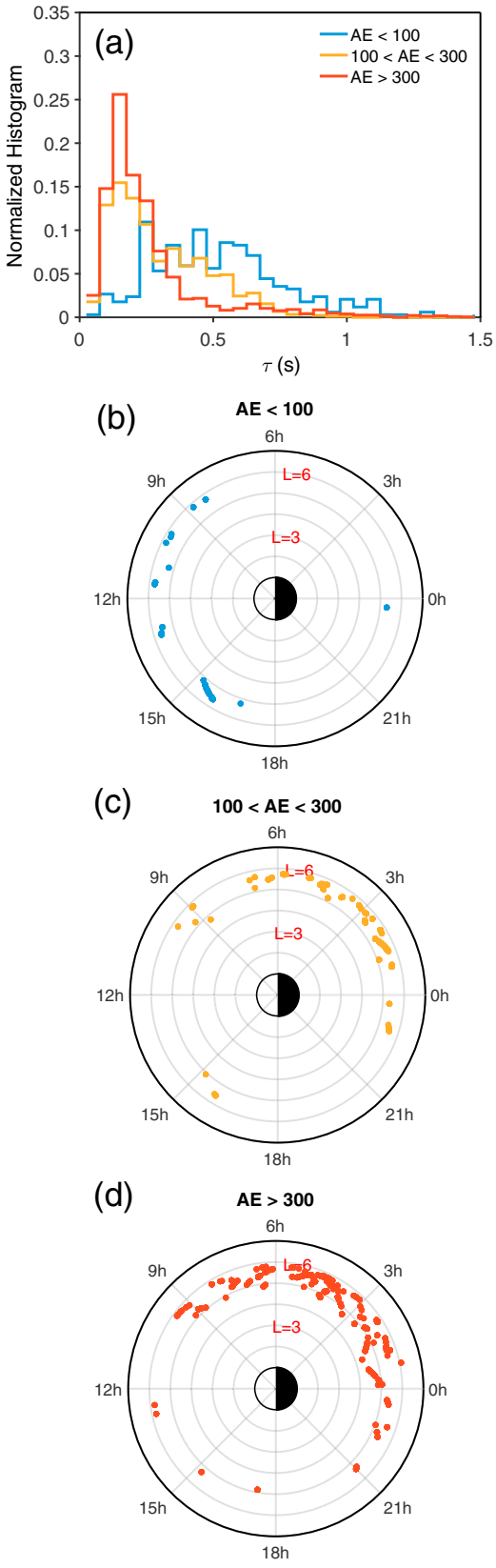

Figure 3. (a) The probability distribution of τ for three different levels of geomagnetic activity characterized by the *AE* index. (b–d) The distribution of events of different geomagnetic activity levels in the MLT-L plane.

by whistler mode waves as electrons drift from nightside to dayside. At the same time, the scattering leads to loss of energetic electrons to the atmosphere, leading to a reduction in the hot electron number density. The chosen A and n_h are therefore qualitatively consistent with observations. The generated chorus elements for two different ξs are shown in Figures 2c and 2d using wave magnetic field recorded at $z = 12c/\Omega_{e0}$ for ξ_N and $z = 24c/\Omega_{e0}$ for ξ_D corresponding to $\lambda = 3°$ for these two ξs. Here c is the speed of light in vacuum, and λ is the latitude. The distance corresponding to $\lambda = 3°$ for a given ξ is calculated, assuming a dipole field, by integrating $dz = LR_p(1 + 3\sin^2\lambda)^{1/2}\cos(\lambda)d\lambda$, where LR_p is obtained from ξ by $LR_p = \sqrt{4.5/\xi}$. The generated chorus element for ξ_N has a larger amplitude compared with that for ξ_D; this is probably related to the larger linear drive required to excite chorus element for ξ_N. The duration of the element for ξ_D is about $2,000\Omega_{e0}^{-1}$, while that for ξ_N is about $1,000\Omega_{e0}^{-1}$. This is consistent with our earlier conjecture that the background magnetic field inhomogeneity is an important factor in determining the duration of chorus elements.

To further test the conjecture using observations, we use TS04 magnetic field model to calculate the inhomogeneity factor for each selected event. We calculate the magnetic field strength B as a function of $\tilde{s}$, which is the distance along the field line from the equator in unit of Earth radius, and model this function using $B = B_0(1 + \tilde{\xi}\tilde{s}^2)$ (Tao, Bortnik, Thorne, Albert, & Angelopoulos, 2012). Here $\tilde{\xi} = 4.5/L^2$ for a dipole field and it is dimensionless. We plot τ as a function of $\tilde{\xi}$ for all events from four sectors in Figure 2e. It is clear that all dayside events have smaller $\tilde{\xi}$ than nightside events, and most of the duskside events have an inhomogeneity $\tilde{\xi} \sim 0.2$, smaller than most dawnside and all nightside events. Typically, these dayside and duskside events have a longer duration than dawnside and nightside events. A few duskside events have a larger inhomogeneity factor, $\tilde{\xi} \sim 0.28$ and ~0.4, and these events have a duration comparable to that of nightside events. For duskside and dawnside events with similar inhomogeneity factor ($\tilde{\xi} \sim 0.2$), their range of duration is also similar. In general, the $\tau - \tilde{\xi}$ relation qualitatively agrees with our earlier conjecture.

However, Figure 2(e) also shows that for a given $\tilde{\xi}$, the duration has a large spread, especially for smaller $\tilde{\xi}$, suggesting that the inhomogeneity factor is not the only parameter that determines the duration. Further detailed theoretical and numerical work are needed to understand what parameters control the duration and the underlying physical mechanism; for example, following the theoretical framework outlined in Chen and Zonca (2016) and Zonca et al. (2017). This is, however, beyond the scope of this study, and we leave it to future work.

3.2. The Dependence of τ on the *AE* Index

Figure 3a shows the dependence of τ on the geomagnetic activity level, characterized by the instantaneous *AE* index. We sort these elements into three categories depending on the *AE* index (quiet: $AE < 100$ nT, moderate: 100 nT $\leq AE \leq$ 300 nT, and strong: $AE >$ 300 nT). During quiet conditions, the duration of most chorus elements are between about $\tau = 0.25$ s and 0.65 s. However, during moderate and active conditions, the distribution of τ is sharply peaked at 0.12 s. Therefore, chorus elements generated during disturbed times have a shorter duration compared with those generated during quiet times.

The dependence of τ on the *AE* index is related to its dependence on MLT. To demonstrate this, we plot the MLT distribution of elements during three

different levels of geomagnetic activity in Figures 3b–3d. It is clear that most chorus elements during quiet times are generated at dayside and duskside, while most of those during more disturbed times ($AE > 100$ nT) are generated at dawnside and nightside. This explains the dependence of τ on the *AE* index. Note that the occurrence pattern of chorus distribution with the *AE* index is fully consistent with previous statistical results reported by Li et al. (2009) and is explained by Tao, Lu, et al. (2014). Therefore, the *AE* dependence of the chorus element duration can be understood in the same way as the dependence of τ on MLT.

3.3. The Relation Between τ and Γ

It is well known that each chorus element consists of so-called subpackets (Crabtree et al., 2017; Santolík et al., 2004). Tao et al. (2017a) suggest that the subpacket is caused by the motion of phase-trapped electrons and that the period of the subpacket is about the typical phase-trapping period (T_{tr}) at generation. The latter fact has also been demonstrated and explained using the so-called sequential triggering process by Shoji and Omura (2013) and Omura and Nunn (2011). Therefore, it is natural to measure τ in terms of the typical phase-trapping period for a given element; that is, $\tau = \alpha T_{tr}$ with α the normalized duration. On the other hand, Vomvoridis et al. (1982) and Omura et al. (2008) have shown that the frequency chirping rate of parallel-propagating chorus waves is related to the trapping frequency $\omega_{tr} = 2\pi/T_{tr}$ by

$$\Gamma = \frac{\partial \omega}{\partial t} = \frac{1}{2}\left(1 - \frac{v_r}{v_g}\right)^{-2} \omega_{\mathrm{tr}}^2, \tag{1}$$

where v_r is the resonant velocity and v_g is the wave group velocity. For cyclotron resonance with lower band parallel-propagating whistler mode waves, $|v_r| = (|\Omega_e| - \omega)/k \sim v_p \sim v_g$, where $v_p = \omega/k$ is the wave phase velocity with k the wave number. Therefore,

$$\Gamma \sim \frac{\omega_{\mathrm{tr}}^2}{\mathcal{O}(10)}. \tag{2}$$

The fact that both τ and Γ are related to ω_{tr} suggest that the two are naturally connected. Therefore, we investigate the relationship between τ and Γ from observation.

The correctness of equation (1) has been demonstrated by several studies (Hikishima & Omura, 2012; Katoh & Omura, 2013; Tao et al., 2017a, 2017b). However, as far as we are aware of, none of previous theoretical or numerical studies about chorus waves have predictions about τ. Therefore, we here try two extremely simplified models of τ to investigate the relation between τ and Γ. The first one is that, for simplicity, $\alpha \equiv \tau/T_{\mathrm{tr}}$ is a constant of order 10; that is,

$$\tau \sim \mathcal{O}(10) T_{\mathrm{tr}} = \mathcal{O}(10)\frac{2\pi}{\omega_{\mathrm{tr}}}, \tag{3}$$

which means that a typical chorus element consists of about 10 subpackets, as frequently shown in observation and simulation, regardless of the frequency chirping rate. Equations (2) and (3) lead to

$$\tau \sim \mathcal{O}(10)\frac{2\pi}{\sqrt{\mathcal{O}(10)\Gamma}} \sim \mathcal{O}(10)\Gamma^{-1/2}. \tag{4}$$

The second approach is to assume that the frequency range of chorus elements $\Delta\omega \approx \tau\Gamma$ is roughly the same for all chorus elements, which could be due to, for example, the presence of the gap at $0.5\Omega_{e0}$. Therefore,

$$\tau \propto \Gamma^{-1}. \tag{5}$$

These two simplified models give different scaling laws for τ as a function of Γ. Both of them will be tested using observation.

Figure 4a shows the distribution of normalized duration ($\tau\Omega_{e0}$) for each chorus element with respect to the normalized frequency chirping rate (Γ/Ω_{e0}^2). A linear fitting to all data points is performed and shown by the red line. The fitting gives $\tau\Omega_{e0} = 0.04(\Gamma/\Omega_{e0}^2)^{-1.1}$. For comparison, we also plot $\tau = 30(\Gamma/\Omega_{e0}^2)^{-0.5}$ in green; the constant factor 30 is chosen for the reference line to match the range of data. Clearly, observation results support equation (5), which means that the frequency range of chorus elements is roughly the same for all chorus elements. This is further demonstrated in Figure 4b, where we plot the normalized frequency range $\Delta\omega/\Omega_{e0}$ as a function of Γ/Ω_{e0}^2. Most chorus elements have a frequency range of about $0.05–0.15\Omega_{e0}$, regardless of the chirping rate. The typical starting and ending frequencies of chorus elements are shown

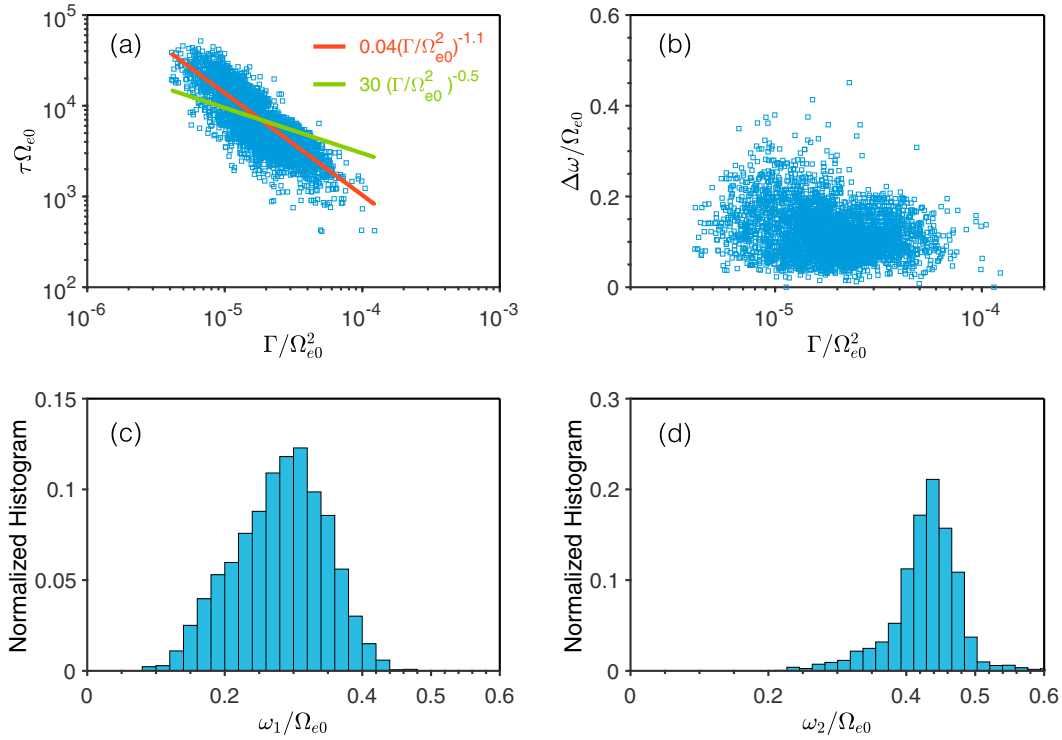

Figure 4. (a) The distribution of observed normalized chorus element duration ($\tau\Omega_{e0}$) versus the normalized frequency chirping rate (Γ/Ω_{e0}^2). The red line is the corresponding linear fitting of these elements, and the green line is a model estimate that $\tau \propto \Gamma^{-1/2}$. (b) The distribution of normalized frequency bandwidth ($\Delta\omega/\Omega_{e0}$) versus the normalized frequency chirping rate (Γ/Ω_{e0}^2). The distribution of the normalized (c) starting and (d) ending frequencies of all chorus elements.

in Figures 4c and 4d. These plots demonstrate that the selected chorus elements typically have a starting frequency near about $0.25-0.35\Omega_{e0}$ and an ending frequency near $0.45\Omega_{e0}$. Only a small percentage of chorus elements have an ending frequency larger than $0.5\Omega_{e0}$.

Another implication of the relation between τ and Γ is about the relation between τ and the wave amplitude at generation, δB. Because the wave amplitude can change significantly after generation even if we only consider events with |MLAT| less than 3°, the dependence of τ on the wave amplitude at generation cannot be investigated directly. However, because $\Gamma \propto \omega_{tr}^2 \propto \delta B$, and $\tau \propto \Gamma^{-1}$, our study suggests that $\tau \propto 1/\delta B$.

4. Summary and Discussion

In this work, we analyzed the distribution of lower-band rising tone chorus element duration. Our statistical analysis demonstrates that chorus elements from nightside and dawnside typically have a shorter duration than those from dayside and duskside by about a factor of 2 to 4. Combining Van Allen Probes observation and the DAWN code simulation, we suggest that a possibly important factor in controlling the observed MLT dependence of the duration is the background magnetic field inhomogeneity. We also analyzed the dependence of τ on the geomagnetic activity level characterized by the *AE* index. We showed that the duration in general decreases with increasing level of geomagnetic activity, and this is consistent with the dependence of τ on MLT and the occurrence pattern of chorus waves. We then investigated the correlation between the duration and the frequency chirping rate. We showed from observation that $\tau \sim \Gamma^{-1}$, suggesting that statistically, the frequency range of lower-band chorus elements should roughly be the same, regardless of the duration or the frequency chirping rate. Therefore, the background magnetic field inhomogeneity factor is not a key factor in determining the frequency range of chorus elements. The τ-Γ relation also suggests that $\tau \propto 1/\delta B$. We did not investigate the dependence of τ on *L* shell because of the limited *L* shell coverage of our data set.

Finally, we remark that further theoretical and numerical studies are needed to understand fully what controls the duration of chorus elements and the underlying physical mechanism. This mechanism might be related

to the one that stops chirping of chorus, as shown by the DAWN code simulation. If this is the case, we will also need to understand what controls the frequency range of chorus elements and why $\tau \propto 1/\Gamma$. On the other hand, the mechanism might be related to the one that produces the gap near $0.5\Omega_{e0}$. In this case, it is relatively easy to explain the τ-Γ relation, as discussed in previous sections, and the dependence of τ on MLT, which is because of the dependence of Γ on MLT. Note that the mechanism for the gap at $0.5\Omega_{e0}$ might be different from the one for the stopping of chirping in case of no gap, and it is a hot research topic by itself. While we cannot determine which mechanism is responsible to explain our observation, our study should be helpful to the further development of a self-consistent theory about chorus generation.

Acknowledgments
We acknowledge the Van Allen Probes data from the EMFISIS instrument obtained from https://emfisis.physics.uiowa.edu/data/index and the Space Physics Data Facility at the NASA Goddard Space Flight Center for providing the OMNI2 data (ftp://spdf.gsfc.nasa.gov/pub/data/omni/omni_cdaweb/). This work was supported by NSFC grants (41474142, 41631071, and 41674174), NMCFERP, and US DoE.

References

Albert, J. M., Tao, X., & Bortnik, J. (2012). Aspects of nonlinear wave-particle interactions. In D. Summers, et al. (Eds.), *Dynamics of the Earth's radiation belts and inner magnetosphere, Geophysical Monograph Series* (Vol. 199, pp. 255–264). Washington, DC: American Geophysical Union. https://doi.org/10.1029/2012GM001324

Artemyev, A. V., Krasnoselskikh, V. V., Agapitov, O. V., Mourenas, D., & Rolland, G. (2012). Non-diffusive resonant acceleration of electrons in the radiation belts. *Physics of Plasmas*, *19*(122), 901.

Bell, T. F. (1984). The nonlinear gyroresonance interaction between energetic electrons and coherent VLF waves propagating at an arbitrary angle with respect to the Earth's magnetic field. *Journal of Geophysical Research*, *89*(A2), 905–918.

Bortnik, J., Thorne, R. M., & Inan, U. S. (2008). Nonlinear interaction of energetic electrons with large amplitude chorus. *Geophysical Research Letters*, *35*, L21102. https://doi.org/10.1029/2008GL035500

Burtis, W. J., & Helliwell, R. A. (1975). Magnetospheric chorus: Amplitude and growth rate. *Journal of Geophysical Research*, *80*(22), 3265–3270. https://doi.org/10.1029/JA080i022p03265

Burtis, W. J., & Helliwell, R. A. (1976). Magnetospheric chorus: Occurrence patterns and normalized frequency. *Planetary and Space Science*, *24*(11), 1007–1010. https://doi.org/10.1016/0032-0633(76)90119-7

Cattell, C., Wygant, J. R., Goetz, K., Kersten, K., Kellogg, P. J., von Rosenvinge, T., … Russell, C. T. (2008). Discovery of very large amplitude whistler-mode waves in Earth's radiation belts. *Geophysical Research Letters*, *35*, L01105. https://doi.org/10.1029/2007GL032009

Chen, L., & Zonca, F. (2016). Physics of Alfvén waves and energetic particles in burning plasmas. *Reviews of Modern Physics*, *88*, 015008. https://doi.org/10.1103/RevModPhys.88.015008

Crabtree, C., Tejero, E., Ganguli, G., Hospodarsky, G. B., & Kletzing, C. A. (2017). Bayesian spectral analysis of chorus subelements from the Van Allen Probes. *Journal of Geophysical Research: Space Physics*, *122*, 6088–6106. https://doi.org/10.1002/2016JA023547

Helliwell, R. A. (1967). A theory of discrete VLF emissions from the magnetosphere. *Journal of Geophysical Research*, *72*(19), 4773–4790. https://doi.org/10.1029/JZ072i019p04773

Hikishima, M., & Omura, Y. (2012). Particle simulations of whistler-mode rising-tone emissions triggered by waves with different amplitudes. *Journal of Geophysical Research*, *117*, A04226. https://doi.org/10.1029/2011JA017428

Horne, R. B., Thorne, R. M., Shprits, Y. Y., Meredith, N. P., Glauert, S. A., Smith, A. J., … Decreau, P. M. E. (2005). Wave acceleration of electrons in the Van Allen radiation belts. *Nature*, *437*, 227–230. https://doi.org/10.1038/nature03939

Inan, U. S., Bell, T. F., & Helliwell, R. A. (1978). Nonlinear pitch angle scattering of energetic electrons by coherent VLF waves in the magnetosphere. *Journal of Geophysical Research*, *83*(A7), 3235–3253.

Katoh, Y., & Omura, Y. (2007). Computer simulation of chorus wave generation in the Earth's inner magnetosphere. *Geophysical Research Letters*, *34*, L03102. https://doi.org/10.1029/2006GL028594

Katoh, Y., & Omura, Y. (2013). Effect of the background magnetic field inhomogeneity on generation processes of whistler-mode chorus and broadband hiss-like emissions. *Journal of Geophysical Research: Space Physics*, *118*, 4189–4198. https://doi.org/10.1002/jgra.50395

Keika, K., Spasojevic, M., Li, W., Bortnik, J., Miyoshi, Y., & Angelopoulos, V. (2012). PENGUIn/AGO and THEMIS conjugate observations of whistler mode chorus waves in the dayside uniform zone under steady solar wind and quiet geomagnetic conditions. *Journal of Geophysical Research*, *117*, A07212. https://doi.org/10.1029/2012JA017708

Kellogg, P. J., Cattell, C. A., Goetz, K., Monson, S. J., & Wilson III, L. B. (2010). Electron trapping and charge transport by large amplitude whistlers. *Geophysical Research Letters*, *37*, L20106. https://doi.org/10.1029/2010GL044845

Kennel, C. F., & Engelmann, F. (1966). Velocity space diffusion from weak plasma turbulence in a magnetic field. *Physics of Fluids*, *9*(12), 2377–2388. https://doi.org/10.1063/1.1761629

Kersten, K., Cattell, C. A., Breneman, A., Goetz, K., Kellogg, P. J., Wygant, J. R., … Roth, I. (2011). Observation of relativistic electron microbursts in conjunction with intense radiation belt whistler-mode waves. *Geophysical Research Letters*, *38*, L08107. https://doi.org/10.1029/2011GL046810

Kessel, R., Fox, N., & Weiss, M. (2013). The radiation belt storm probes (RBSP) and space weather. *Space Science Reviews*, *179*(1–4), 531–543. https://doi.org/10.1007/s11214-012-9953-6

Kletzing, C. A., Kurth, W. S., Acuna, M., MacDowall, R. J., Torbert, R. B., Averkamp, T., … Tyler, J. (2013). The Electric and Magnetic Field Instrument Suite and Integrated Science (EMFISIS) on RBSP. *Space Science Reviews*, *179*, 127–181. https://doi.org/10.1007/s11214-013-9993-6

Li, W., Thorne, R. M., Angelopoulos, V., Bortnik, J., Cully, C. M., Ni, B., … Magnes, W. (2009). Global distribution of whistler-mode chorus waves observed on the THEMIS spacecraft. *Geophysical Research Letters*, *36*, L09104. https://doi.org/10.1029/2009GL037595

Li, W., Thorne, R. M., Nishimura, Y., Bortnik, J., Angelopoulos, V., McFadden, J. P., … Auster, U. (2010). THEMIS analysis of observed equatorial electron distributions responsible for the chorus excitation. *Journal of Geophysical Research*, *115*, A00F11. https://doi.org/10.1029/2009JA014845

Lorentzen, K. R., Blake, J. B., Inan, U. S., & Bortnik, J. (2001). Observations of relativistic electron microbursts in association with VLF chorus. *Journal of Geophysical Research*, *106*(A4), 6017–6027. https://doi.org/10.1029/2000JA003018

Macúšová, E., Santolík, O., Décréau, P., Demekhov, A. G., Nunn, D., & Gurnett, D. A. (2010). Observations of the relationship between frequency sweep rates of chorus wave packets and plasma density. *Journal of Geophysical Research*, *115*, A12257. https://doi.org/10.1029/2010JA015468

Mauk, B., Fox, N. J., Kanekal, S., Kessel, R., Sibeck, D., & Ukhorskiy, A. (2013). Science objectives and rationale for the radiation belt storm probes mission. *Space Science Reviews*, *179*(1–4), 3–27. https://doi.org/10.1007/s11214-012-9908-y

Meredith, N. P., Johnstone, A. D., Szita, S., Horne, R. B., & Anderson, R. R. (1999). "Pancake" electron distributions in the outer radiation belts. *Journal of Geophysical Research*, *104*(A6), 12,431–12,444. https://doi.org/10.1029/1998JA900083

Nishimura, Y., Bortnik, J., Li, W., Thorne, R. M., Lyons, L. R., Angelopoulos, V., … Auster, U. (2010). Identifying the driver of pulsating aurora. *Science*, *330*(6000), 81–84. https://doi.org/10.1126/science.1193186

Nunn, D. (1971). A theory of VLF emissions. *Planetary and Space Science*, *19*, 1141–1167.

Omura, Y., Furuya, N., & Summers, D. (2007). Relativistic turning acceleration of resonant electrons by coherent whistler mode waves in a dipole magnetic field. *Journal of Geophysical Research*, *112*, A06236. https://doi.org/10.1029/2006JA012243

Omura, Y., Katoh, Y., & Summers, D. (2008). Theory and simulation of the generation of whistler-mode chorus. *Journal of Geophysical Research*, *113*, A04223. https://doi.org/10.1029/2007JA012622

Omura, Y., & Nunn, D. (2011). Triggering process of whistler mode chorus emissions in the magnetosphere. *Journal of Geophysical Research*, *116*, A05205. https://doi.org/10.1029/2010JA016280

Reeves, G. D., Spence, H. E., Henderson, M. G., Morley, S. K., Friedel, R. H. W., Funsten, H. O., … Niehof, J. T. (2013). Electron acceleration in the heart of the Van Allen radiation belts. *Science*, *341*(6149), 991–994. https://doi.org/10.1126/science.1237743

Santolík, O., Gurnett, D. A., Pickett, J. S., Parrot, M., & Cornilleau-Wehrlin, N. (2004). A microscopic and nanoscopic view of storm-time chorus on 31 March 2001. *Geophysical Research Letters*, *31*, L02801. https://doi.org/10.1029/2003GL018757

Santolík, O., Kletzing, C. A., Kurth, W. S., Hospodarsky, G. B., & Bounds, S. R. (2014). Fine structure of large-amplitude chorus wave packets. *Geophysical Research Letters*, *41*, 293–299. https://doi.org/10.1002/2013GL058889

Santolík, O., Nemec, F., Gereová, K., Macúšová, E., Conchy, Y., & Cornilleau-Wehrlin, N. (2004). Systematic analysis of equatorial noise below the lower hybrid frequency. *Annales Geophysicae*, *12*, 2587–2595.

Shoji, M., & Omura, Y. (2013). Triggering process of electromagnetic ion cyclotron rising tone emissions in the inner magnetosphere. *Journal of Geophysical Research: Space Physics*, *118*, 5553–5561. https://doi.org/10.1002/jgra.50523

Shue, J.-H., Hsieh, Y.-K., Tam, S. W., Wang, K., Fu, H. S., Bortnik, J., … Pi, G. (2015). Local time distributions of repetition periods for rising tone lower band chorus waves in the magnetosphere. *Geophysical Research Letters*, *42*, 8294–8301. https://doi.org/10.1002/2015GL066107

Soto-Chavez, A. R., Wang, G., Bhattacharjee, A., Fu, G. Y., & Smith, H. M. (2014). A model for falling-tone chorus. *Geophysical Research Letters*, *41*, 1838–1845. https://doi.org/10.1002/2014GL059320

Spasojevic, M., & Inan, U. S. (2010). Drivers of chorus in the outer dayside magnetosphere. *Journal of Geophysical Research*, *115*, A00F09. https://doi.org/10.1029/2009JA014452

Tao, X. (2014). A numerical study of chorus generation and the related variation of wave intensity using the DAWN code. *Journal of Geophysical Research: Space Physics*, *119*, 3362–3372. https://doi.org/10.1002/2014JA019820

Tao, X., & Bortnik, J. (2010). Nonlinear interactions between relativistic radiation belt electrons and oblique whistler mode waves. *Nonlinear Processes in Geophysics*, *17*, 599–604. https://doi.org/10.5194/npg-17-599-2010

Tao, X., Bortnik, J., Albert, J. M., Thorne, R. M., & Li, W. (2014). Effects of discreteness of chorus waves on quasilinear diffusion-based modeling of energetic electron dynamics. *Journal of Geophysical Research: Space Physics*, *119*, 8848–8857. https://doi.org/10.1002/2014JA020022

Tao, X., Bortnik, J., Thorne, R. M., Albert, J., & Li, W. (2012). Effects of amplitude modulation on nonlinear interactions between electrons and chorus waves. *Geophysical Research Letters*, *39*, L06102. https://doi.org/10.1029/2012GL051202

Tao, X., Li, W., Bortnik, J., Thorne, R. M., & Angelopoulos, V. (2012). Comparison between theory and observation of the frequency sweep rates of equatorial rising tone chorus. *Geophysical Research Letters*, *39*, L08106. https://doi.org/10.1029/2012GL051413

Tao, X., Lu, Q., Wang, S., & Dai, L. (2014). Effects of magnetic field configuration on the day-night asymmetry of chorus occurrence rate: A numerical study. *Geophysical Research Letters*, *41*, 6577–6582. https://doi.org/10.1002/2014GL061493

Tao, X., Thorne, R. M., Li, W., Ni, B., Meredith, N. P., & Horne, R. B. (2011). Evolution of electron pitch-angle distributions following injection from the plasma sheet. *Journal of Geophysical Research*, *116*, A04229. https://doi.org/10.1029/2010JA016245

Tao, X., Zonca, F., & Chen, L. (2017a). Identify the nonlinear wave-particle interaction regime in rising tone chorus generation. *Geophysical Research Letters*, *44*, 3441–3446. https://doi.org/10.1002/2017GL072624

Tao, X., Zonca, F., & Chen, L. (2017b). Investigations of the electron phase space dynamics in triggered whistler wave emissions using low noise δf method. *Plasma Physics and Controlled Fusion*, *59*(9), 094001.

Thorne, R. M., Li, W., Ni, B., Ma, Q., Bortnik, J., Chen, L., … Kanekal, S. G. (2013). Rapid local acceleration of relativistic radiation-belt electrons by magnetospheric chorus. *Nature*, *504*, 411–414. https://doi.org/10.1038/nature12889

Thorne, R. M., Ni, B., Tao, X., Horne, R. B., & Meredith, N. P. (2010). Scattering by chorus waves as the dominant cause of diffuse auroral precipitation. *Nature*, *467*, 943–946. https://doi.org/10.1038/nature09467

Trakhtengerts, V. Y. (1995). Magnetosphere cyclotron maser: Backward wave oscillator generation regime. *Journal of Geophysical Research*, *100*(A9), 17,205–17,210. https://doi.org/10.1029/95JA00843

Tsurutani, B. T., & Smith, E. J. (1974). Postmidnight chorus: A substorm phenomenon. *Journal of Geophysical Research*, *79*(1), 118–127.

Tsyganenko, N., & Sitnov, M. (2005). Modeling the dynamics of the inner magnetosphere during strong geomagnetic storms. *Journal of Geophysical Research*, *110*, A03208. https://doi.org/10.1029/2004JA010798

Vomvoridis, J. L., Crystal, T. L., & Denavit, J. (1982). Theory and computer simulations of magnetospheric very low frequency emissions. *Journal of Geophysical Research*, *87*(A3), 1473–1489. https://doi.org/10.1029/JA087iA03p01473

Wilson III, L. B., Cattell, C. A., Kellogg, P. J., Wygant, J. R., Goetz, K., Breneman, A., & Kersten, K. (2011). The properties of large amplitude whistler mode waves in the magnetosphere: Propagation and relationship with geomagnetic activity. *Geophysical Research Letters*, *38*, L17107. https://doi.org/10.1029/2011GL048671

Zonca, F., Tao, X., & Chen, L. (2017). Nonlinear wave-particle dynamics in chorus excitation. In *44th EPS Conference on Plasma Physics* (Vol. 41F). Northern Ireland: EPS, Belfast.